doi:10.1016/j.jmb.2011.04.014 J. Mol. Biol. (2011) 412, 882–893

Contents lists available at www.sciencedirect.com

Journal of Molecular Biology

journal homepage: http://ees.elsevier.com.jmb

Helix 12 Dynamics and Thyroid Hormone Receptor Activity: Experimental and Molecular Dynamics Studies of Ile280 Mutants

Paulo C. T. Souza[1], Gustavo B. Barra[2], Lara F. R. Velasco[2], Isabel C. J. Ribeiro[2], Luiz A. Simeoni[2], Marie Togashi[2], Paul Webb[3], Francisco A. R. Neves[2], Munir S. Skaf[1], Leandro Martínez[4] and Igor Polikarpov[4]*

[1]*Institute of Chemistry, State University of Campinas, Campinas, SP, Brazil*
[2]*Faculdade de Ciências da Saúde, Universidade de Brasília, Brasília, DF, Brazil*
[3]*The Methodist Hospital Research Center, Houston, TX, USA*
[4]*Instituto de Física de São Carlos, Universidade de São Paulo, Av. Trabalhador Sãocarlense 400, 13560-970 São Carlos, SP, Brazil*

Received 18 January 2011; received in revised form 6 April 2011; accepted 6 April 2011
Available online 21 April 2011

Edited by D. Case

Keywords:
nuclear hormone receptor; thyroid; cofactor recruitment; molecular dynamics simulations

Nuclear hormone receptors (NRs) form a family of transcription factors that mediate cellular responses initiated by hormone binding. It is generally recognized that the structure and dynamics of the C-terminal helix 12 (H12) of NRs' ligand binding domain (LBD) are fundamental to the recognition of coactivators and corepressors that modulate receptor function. Here we study the role of three mutations in the I280 residue of H12 of thyroid hormone receptors using site-directed mutagenesis, functional assays, and molecular dynamics simulations. Although residues at position 280 do not interact with coactivators or with the ligand, we show that its mutations can selectively block coactivator and corepressor binding, and affect hormone binding affinity differently. Molecular dynamics simulations suggest that ligand affinity is reduced by indirectly displacing the ligand in the binding pocket, facilitating water penetration and ligand destabilization. Mutations I280R and I280K link H12 to the LBD by forming salt bridges with E457 in H12, stabilizing H12 in a conformation that blocks both corepressor and coactivator recruitment. The I280M mutation, in turn, blocks corepressor binding, but appears to enhance coactivator affinity, suggesting stabilization of H12 in agonist conformation.

Introduction

Thyroid hormone receptors (TRs) are transcription factors modulated by thyroid hormone binding.[1–3] They belong to the nuclear hormone receptor (NR) superfamily, one of the major targets of pharmaceuticals comprising receptors for estrogens and its analogs, corticosteroids, and retinoic acid and derivatives, to mention a few. NRs contain three domains: a variable N-terminal domain with unknown structure, a DNA binding domain that recognizes DNA response elements, and a ligand

*Corresponding author. E-mail address: ipolikarpov@ifsc.usp.br.

Abbreviations used: NR, nuclear hormone receptor; H12, helix 12; LBD, ligand binding domain; TR, thyroid hormone receptor; RXR, retinoid X receptor; RAR, retinoic acid receptor; MD, molecular dynamics; GST, glutathione *S*-transferase; MSA, multiple sequence alignment; PDB, Protein Data Bank; CG, conjugate gradient.

binding domain (LBD) that selectively recognizes hormones and contains interfaces for dimerization and cofactor recruitment.[4–10]

The structure and dynamics of the LBD are essential for transcription regulation. It is currently accepted that in the absence of ligand, the C-terminal helix [helix 12 (H12)] of the LBD is positioned such that it exposes an interface for corepressor binding. In positively regulated genes, the NR inhibits gene transcription while bound to the corepressor. Ligand binding perturbs the dynamic equilibrium of H12, which adopts a novel preferential orientation that favors coactivator—instead of corepressor—recruitment. Dissociation of corepressor and binding of coactivator initiate transcription.[8–10] Thus, H12 conformation and dynamics are key factors that modulate ligand-dependent transcription regulation.

The dynamics of H12 was initially believed to involve its detachment from the body of the LBD, as exemplified by apo retinoid X receptor (RXR) and holo retinoic acid receptor (RAR) crystallographic structures.[11,12] The recruitment of corepressors and coactivators with specific H12 conformations suggests that the movements of H12 are more subtle, as shown in Fig. 1, and are mostly determined by preferential orientations H12 assumes while docked to the surface of the LBD. Ligand entry and exit may occur through subtle movements of H12 or other structural elements. Other crystal structures of apo-LBDs,[13–17] the constitutive activity of receptors,[18–21] molecular dynamics (MD) computer simulation studies,[22–27] and hydrogen–deuterium exchange experiments[28–34] support the view of a dynamic but compact LBD in which H12 can assume both corepressor-favorable and coactivator-favorable conformations in the presence or in the absence of ligand, but with different populations in each case.

In TRs, corepressor and coactivator interfaces overlap and are formed by residues V284, K288, I302, and K306 from helices 3, 5, and 6 (residue numbering according to TRβ isoform). The corepressor binding surface is further complemented by residues T277, I280, T281, V283, and C309, which also belong to helices 3, 5, and 6 but are spatially closer to H12 in holo-TR, whereas the coactivators require residues L454 and E457 from H12 to interact with TR.[35–37]

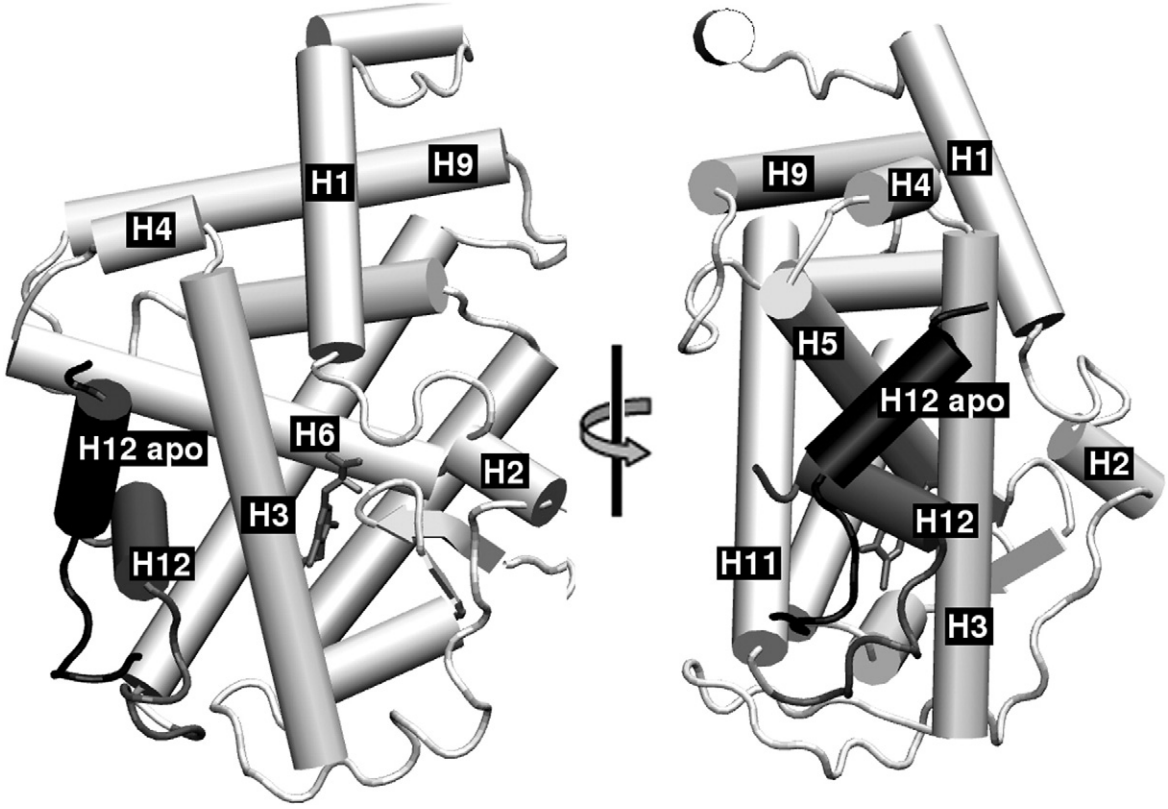

Fig. 1. Structure models of TRβ based on X-ray diffraction data (holo model, gray; PDB ID: 3GWS) and hydrogen–deuterium exchange (apo model; black) suggesting conformational rearrangements through which H12 undergoes ligand binding. The displacement of H12 from the holo conformation results in the exposure of the corepressor binding surface.

H12 is docked over residues I280, V283, and C309 in holo-TR structures, so that corepressor binding requires a conformational shift of H12 from this position. The role of these three residues (I280, V283, and C309) in coactivator and corepressor binding is essential for the comprehension of H12 conformational equilibrium and dynamics. As coactivator—but not corepressor—binding is dependent on direct interactions with H12, deletion of H12 blocks coactivator interactions but increases corepressor association by exposing its interaction surface.[37] Some mutants in this region are also linked to resistance-to-thyroid-hormone syndrome,[38–40] which is usually associated with reduced transcriptional activity and reduced hormone affinity for the receptor.[41]

Here, we report an experimental and computational study of the effects of mutations I280M, I280R, and I280K on the association of coactivators and corepressors, heterodimerization, and ligand affinity. We show that different mutations at position 280 affect each of these functional characteristics of the receptors differently, and MD simulations provide the structural basis for such differential effects.

Results and Discussion

Mutants impair transcriptional activity

Reporter gene assays were used to probe the transcriptional activities of native and mutant I280M, I280R, I280K, F451X, and I280K/F451X. Only mutant I280M preserved significant levels of transcriptional activity relative to wild-type TRβ, as shown in Fig. 2a–c. The relative transcriptional activity is response-element-dependent for each mutant: I280M preserved about 82% of native activity in DR4, 42% of native activity in F2, and 63% of native activity in TREpal. Activation promoted by mutants I280R, I280K, F451X, and I280R/F451X was significantly impaired and similar to basal transcription activity.

Mutants modulate affinity for coactivators and corepressors

As transcriptional activity is dependent on corepressor dissociation and coactivator binding, we

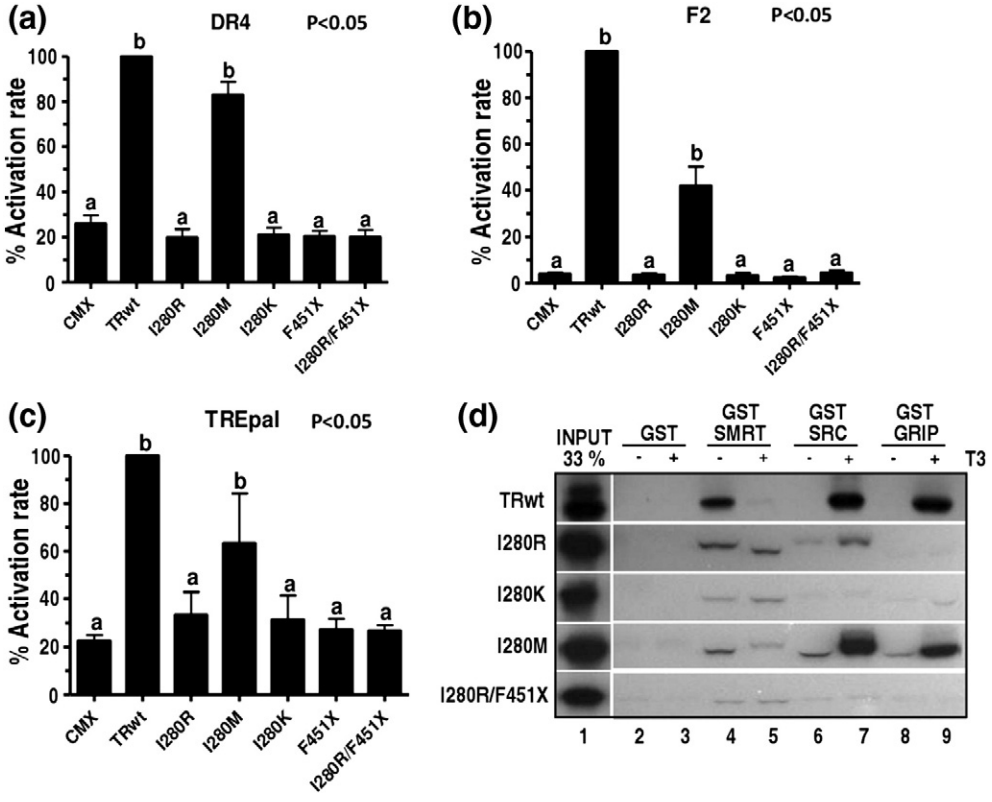

Fig. 2. Transcription activation upon different DNA response elements and coregulator recruitment promoted by native and mutant TRβ. (a) DR-4. U937 cells were cotransfected with 4 μg of DR-4 LUC and 0.5 μg of the expression vector of TRβ1 wild type and mutants and treated with vehicle or 100 nM T_3. Data represent fold T_3 inductions obtained at each amount of TR expression vector and represent the average of the experiments. (b) As above, with F2-LUC. (c) As above, with Pal-LUC. (d) Pull-down experiments examining the binding of ^{35}S-labeled TRβ1 wild type or mutants to GST-SMRT, GST-SRC, and GST-GRIP protein fragment in the presence or in the absence of 10^{-6} M T_3.

probe the affinity of native TRβ and mutant constructs for the corepressor peptide SMRT and for the coactivator peptides SRC and GRIP. As shown in Fig. 2d, SMRT corepressor dissociation from native TRβ–LBD, as expected, was fully determined by ligand (T_3) binding. At the same time, ligand binding induces coactivator attachment to the LBD. Mutants have different effects on these trends: the I280R mutant preserves decreased SMRT affinity, which is mostly ligand-insensitive (Fig. 2d). The association of coactivators is also significantly perturbed, and residual association with SRC and no association with GRIP resulted. The I280K mutant, in turn, almost completely hampers coactivator and corepressor binding under all conditions. The I280M mutant is mostly unable to recruit the SMRT corepressor, but it conserves coactivator binding with ligand and, furthermore, has some coactivator affinity even in the absence of ligand. Finally, the mutation I280R also hampers corepressor binding in the F451X construct. The F451X construct is known to strongly bind corepressors by completely exposing the corepressor binding surface.[37,42]

The effect of mutations on ligand binding affinity

Ligand binding is fundamental to coactivator recruitment and, thus, to transcriptional activity. Trypsin digestion assays were used to probe the protection promoted by the ligand on the LBD and thus to qualitatively evaluate ligand affinity. LBD protection against trypsin digestion is characterized by the appearance of a 28-kDa fraction on glutathione *S*-transferase (GST) assays, as shown in Fig. 3a. The same fragment is observed for micromolar T_3 concentrations for the I280M mutation, but it is not observed for I280R or I280K. Thus, the latter two mutants appear to fully inhibit ligand binding, even though residues in position 280 do not interact directly with the ligand. The complete removal of H12 (F451X construct) also reduces ligand affinity to undetectable levels, as previously noted.[37,42] T_3 affinities for TRβ and for the I280M mutant were then compared (Fig. 3b and c): $K_d = 0.13$ nM for wild-type TRβ and $K_d = 0.45$ nM for I280M mutant.

In summary, GST experiments show that the affinity of the SMRT corepressor peptide interacts with native or mutant LBDs with the following preference: native TRβ > TRβ-I280M ~ TRβ-I280R > TRβ-I280K. Concerning interactions with the coactivator peptides SRC-1 and GRIP1, the affinity of the I280M mutant is not affected relative to the native state such that the affinities vary as follows: native TRβ = TRβ-I280M > TRβ-I280R > TRβ-I280K. Therefore, different mutations at position 280 affect coactivator and corepressor recruitment differently. Additionally, all mutants impair hormone binding. The affinities of T_3 for I280R and I280K are reduced such that ligand binding could not be detected, and the I280M displayed 29% of native TRβ affinity. At the same time, the native and mutant LBDs heterodimerize with RXR with similar affinities, supporting the correct overall fold of the mutant LBDs (data not shown).

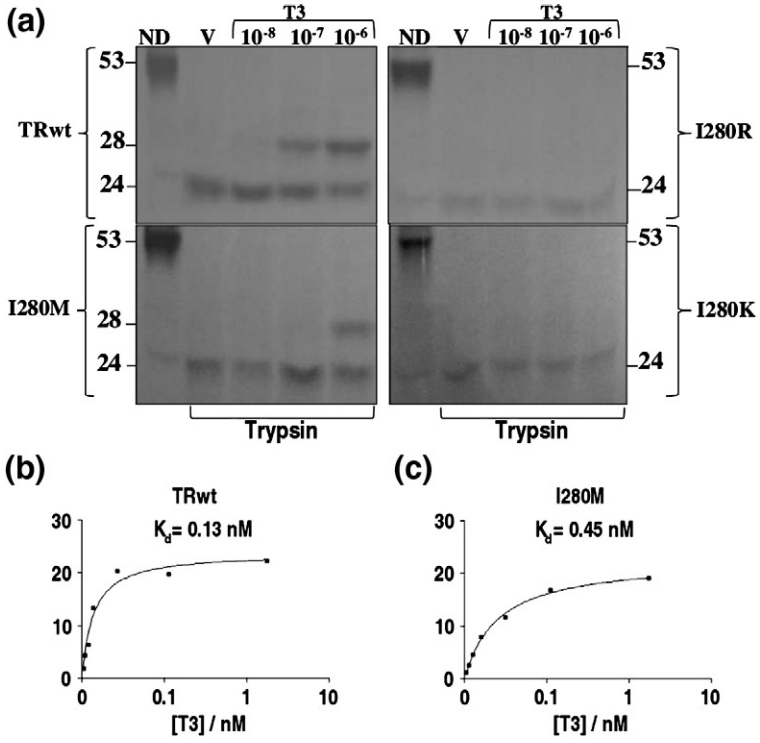

Fig. 3. T_3 binding affinity for native and mutant TRβ1. (a) [^{35}S] TRβ1 or mutants were preincubated with T_3 (10^{-8}, 10^{-7}, and 10^{-6} M) or vehicle (ethanol) for 20 min at room temperature before addition of trypsin (concentration of 10 mg/ml). Proteolytic digestions were carried out at 37 °C for 10 min, and then samples were denatured and electrophoresed on SDS polyacrylamide gel. The 28-kDa band represents the T_3-protected TRβ1 fragment. Binding of [^{125}I]T_3 to full-length TRβ1wt (b) and I280M (c) mutant produced by *in vitro* translation.

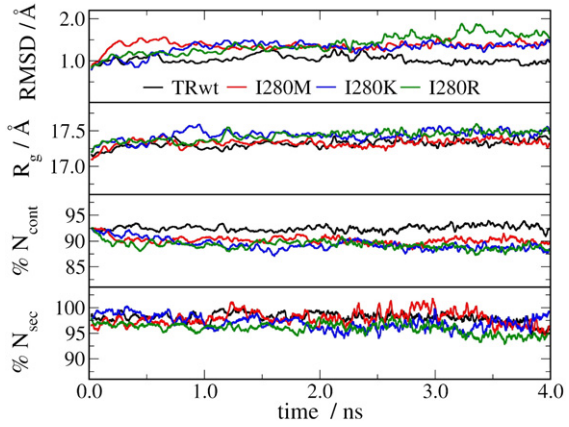

Fig. 4. Global structural features of the LBD through simulations: RMSDs of C^{α} atoms (RMSD), radius of gyration (R_g), percentage of native contacts (% N_{cont}), and percentage of secondary structure (% N_{sec}).

Structural basis for perturbations on cofactor recruitment

The mutations at position 280 affect both binding affinity and the direct interactions of H12 with the LBD core; thus, there are multiple possible interpretations for their effect on coactivator recruitment. The deletion of H12 hampers coactivator binding, so that mutations that fully destabilize this helix should have the same effect. Also, it is clear that I280R and I280K mutations disrupt direct corepressor–LBD interactions, which should be hydrophobic at position 280. The observed lack of SMRT affinity for F451X/I280K supports this interpretation. However, the destabilization of H12 is not the only possible explanation for mutant effects, as MD simulations suggest. Indeed, trapping H12 in a conformation that blocks both coactivator and corepressor surfaces would result in similar experimental observations.

MD simulations support the experimental observation that the overall fold of the LBD is not altered upon mutations of residue I280, as shown in Figs. 4 and 5a. There is a small increase in RMSD from the native structure, never surpassing 2.0 Å for any mutant. The radii of gyration and the α-helical contents of the simulated mutants remain essentially identical with those of the native LBD. There is, however, a small but systematic loss of native contacts for all three mutants relative to the native TRβ structure: mutants lose about 5–8% native contacts during the course of the simulations.

The structural basis of the effect of I280 mutations on cofactor recruitment can be deduced from the analysis of H12 structure and dynamics. As shown in Fig. 5b, there is a significant displacement of H12 in mutants I280R and I280K, but not I280M, relative

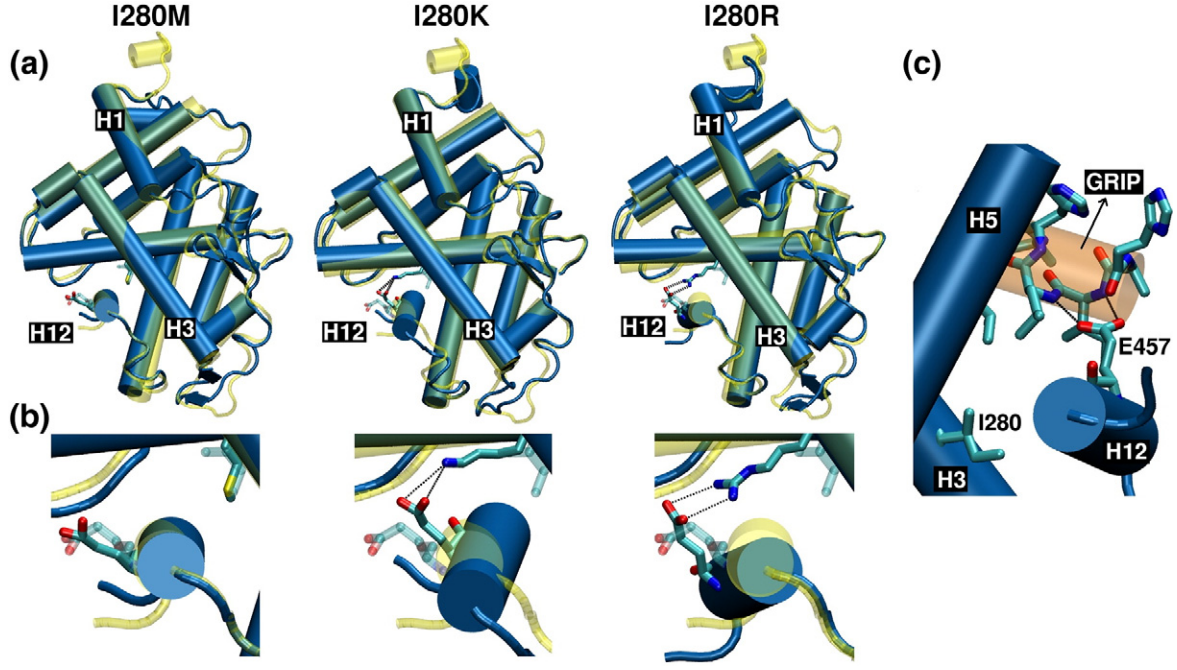

Fig. 5. Average structures from MD simulations. (a) The global folds of native and mutants are similar, but with significant perturbations of the H12 position in I280K and I280R mutants. (b) Detail of the movements of H12 and the interaction of Glu457, from H12, with mutant residues Lys and Arg in position 280. (c) Coactivator binding to the LBD is dependent on the interaction of Glu457 with the main chain of the coactivator peptide, as observed in crystallographic models (PDB ID: 1BSX).[43] Mutants I280K and I280R compete with these interactions, destabilizing coactivator association.

to its position in native holo-TRβ. The position of H12 in this holo model forms the coactivator binding surface such that perturbations of this position should impair coactivator recruitment. Indeed, as observed experimentally, coactivator recruitment is impaired by mutations I280R and I280K, but not I280M, consistent with the displacements of H12 in each case. The perturbation of H12 position in I280R and I280K occurs, however, not by the introduction of steric clashes that destabilize H12. On the contrary, Arg and Lys residues at position 280 form a stable salt bridge with H12 residue Glu457 that is located on the TR–LBD surface and away from the ligand binding pocket, as shown in Fig. 5b. This salt bridge introduces a restraint on the position of H12 relative to the LBD, displacing it from its functional position. The displacement of H12 is not the only factor affecting coactivator affinity for the LBD of I280R and I280K: coactivator binding, as observed in crystallographic models (Fig. 5c), depends on the direct interactions of Glu457 with the coactivator peptide backbone.[43] Therefore, substituting I280 with basic residues, more than simply perturbing H12 position, causes them to compete for the negatively charged Glu457, reducing one of the main interactions of the coactivator peptide with the LBD. TR coactivator recruitment measurements and functional assays with the E457A mutant already confirm the importance of this residue.[40] Substitution I280M, in turn, does not perturb the H12 position because isoleucine and methionine residues share similar volumes and are both hydrophobic. The competition of the Met residue for Glu457 does not occur, thus preserving coactivator binding affinity for the LBD.

The interpretation of corepressor binding affinity differences has to be indirect, as there are no crystal structures for corepressor-bound TRs or apo-TRs (only a preliminary low-resolution model exists based on results from hydrogen–deuterium exchange experiments and high-temperature MD simulations).[34] It is known, however, that corepressor binding requires the displacement of H12 from the holo-LBD position and docking in an alternative conformation that exposes, for instance, residue I280. With this in mind, we propose that the strong interactions that R280 and K280 form with Glu457 impair corepressor recruitment by not allowing H12 to assume the position that establishes the corepressor binding surface. Additionally, the direct hydrophobic contact between corepressor and I280 is lost by apolar-to-polar substitution. This direct mechanism is consistent with the reduced corepressor affinity of the F451X/I280K construct. At the same time, the I280M mutation also impairs corepressor recruitment experimentally, and no alteration in H12 position was observed. It is possible that a Met residue in position 280 promotes some degree of stabilization of the H12 native holo conformation, thus also hampering the formation of the corepressor binding surface. This is consistent with the increase in the coactivator binding affinity of I280M relative to wild-type TRβ, particularly in the absence of ligand. As the interaction energies involved in hydrophobic interactions are more subtle and as no alterations in H12 position or dynamics were observed, further investigations are required to confirm this hypothesis.

H12 stabilization in a closed conformation has also been suggested for other NRs. For example, different mutations in residue Y537, located in H12 of estrogen receptor α, modulate transcriptional activity, coregulator recruitment, and ligand association/dissociation rates. These features are associated with H12 stabilization in the agonist conformation in the apo estrogen receptor α.[44–46] The same interpretation was proposed for isoforms β and γ of RAR. A few differences in residues in helix 3 and in the C-terminal extension of H12 relative to the RARα isoform are associated with a reduced interaction with corepressors and the observation of constitutive transcriptional activity.[47,48] In addition, two mutants in H12 (L468A and E471A) of the peroxisome proliferator activator receptor have been shown to elicit similar behaviors.[49]

Molecular interpretation of mutation effects on ligand affinity

Experimentally, all three I280M, I280R, and I280K mutations reduce T_3 binding affinity. T_3 affinity for I280M mutant is about 29% of the affinity for native LBD, whereas no detectable ligand binding could be observed for I280R and I280K. Since the residues at position 280 do not interact with the ligand, the effect of the mutations on ligand binding affinity must be indirect. Figure 6 displays structural and energetic features of T_3 in the binding pocket of native and mutant structures. The position of the ligand relative to H12 (as measured by the distance between ligand and H12 residues) is not perturbed, except for the I280K mutation (Fig. 6a). Even in this case, the drift is gradually restored to the initial relative orientation between T_3 and H12. However, movements of H12 triggered by the mutations displace the ligand and affect its contact with the arginine residues of the β-hairpin, located on the opposite side of the binding pocket. The β-hairpin–T_3 distance indicates that the ligand shifts by about 2 Å from the arginines for all mutants relative to the native structure.

This conformational adaptation affects both ligand–protein interactions and the hydration level of the ligand in the binding pocket. The LBD–T_3 interactions in the cases of I280R and I280K, and for the I280M mutant to a lesser extent, turn out weaker than that of the native structure, as shown in Fig. 6b. Up to seven water molecules

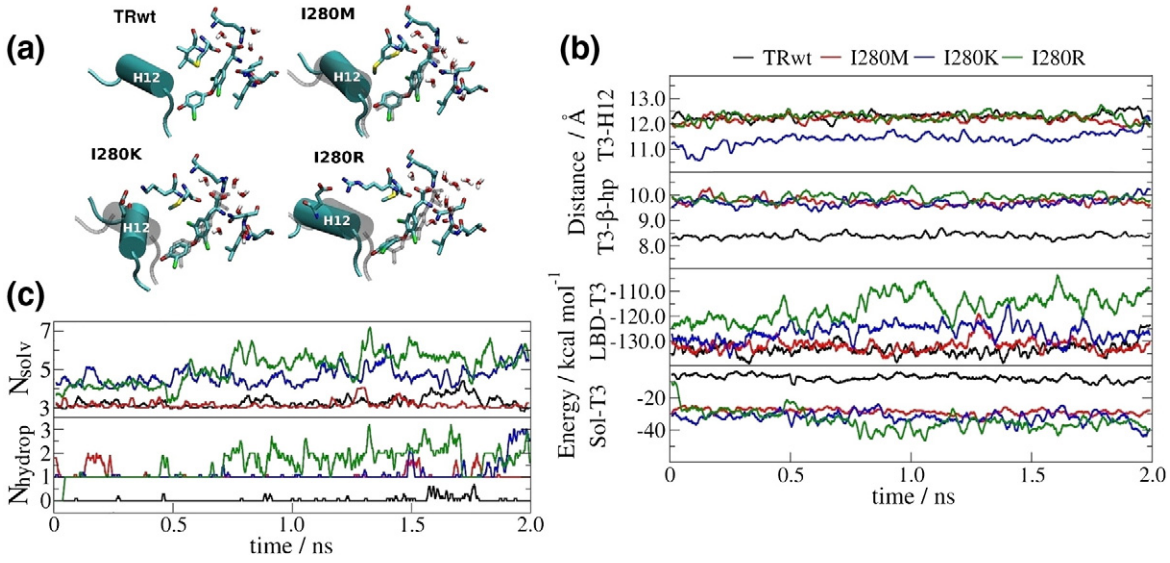

Fig. 6. Displacements of H12 indirectly result in perturbations of the ligand binding pocket, allowing water permeation. (a) Representative snapshots from the simulations showing the movements of H12 water insertion. (b) Distances of T_3 to H12 (T_3–H12) and the β-hairpin (T_3–β-hp), and interaction energies with the LBD (LBD–T_3) and water molecules (Sol–T_3). (c) Number of water molecules solvating T_3 (N_{solv}) and, in particular, its hydrophobic body (N_{hydrop}), which may destabilize ligand binding.

penetrate the binding pocket for the I280R and I280K mutants and increase ligand–solvent interactions (Fig. 6c). Further inspection of ligand hydration inside the binding pocket reveals that up to three of these molecules are in contact with the hydrophobic body of T_3. No extra water molecule, relative to the native structure, occupies the binding pocket for I280M. However, whereas ligand–water interactions in the native LBD occur solely via the ligand's hydrophilic head, the increased flexibility of the I280M mutant binding pocket allows water to interact with the aromatic rings of T_3 in I280M.

The displacement of H12 in mutants induces some repositioning of the ligand in the binding pocket, and T_3–β-hairpin hydrophilic contacts are replaced by interactions with water molecules. The position of T_3 relative to H12 is preserved because hydrophobic contacts are largely maintained within the binding pocket. The ligand becomes loosely attached to the binding pocket, and water molecules are allowed to interact with its hydrophobic residues. The number of water molecules that can penetrate the binding pocket and interact with the hydrophobic parts of T_3 is larger for I280R and I280K mutations than for I280M because the perturbations that the former mutations promote on the H12 structure are larger. The simulations suggest that the observed lower ligand binding affinity of the mutants relative to the native structure stems from a combination of these effects, particularly from the partial destabilization of ligand–LBD hydrophobic contacts due to water penetration into the hydrophobic core of the binding pocket. Thus, structural perturbations of H12 can affect ligand affinity indirectly by displacing the ligand in the binding pocket even if direct ligand–H12 interactions are preserved. Interactions with water molecules in the binding pocket seem to be important to the affinity, selectivity, dissociation, and association of ligands in TRs.[23,25,50,51]

Mutants in the same region in other NRs may have similar effects on ligand binding affinity. However, multiple sequence alignment (MSA) of the TR-like subfamily shows distinct sequence patterns in the I280 region (343 MSA position),[52] which would indicate differentiation of behaviors between receptors. For example, at the same sequence position, V293A mutation in peroxisome proliferator activator receptor γ does not impair receptor functions,[53] whereas double mutations in RARs (one of them at the same MSA position) can change the ligand affinity and selectivity for different isoforms.[54]

Conclusions

The conformation and mobility of NRs' H12 are key structural factors affecting NR transcriptional activity. H12 is mobile and assumes different preferential conformations in the presence and in the absence of ligand. However, the few structural models of apo-LBDs and limited direct experimental information on H12 and LBD dynamics result in the incomplete comprehension of relationships between NR dynamics and function. Here, we address the

effects of the I280 mutants of the LBD of TR to further understand the relationships between perturbations of H12 position and TR function. We have shown that I280 mutations to positively charged residues impair ligand, corepressor, and coactivator binding. This can be explained by two mechanisms: (1) the complete destabilization of H12 position relative to LBD, with total exposure of residues at position 280, consistent with a similar loss of functionality of the complete deletion of H12; and (2) the stabilization of H12 in alternative, but incorrectly docked, conformations in I280K and I280R, which results from the formation of a salt bridge between the residue side chain at position 280 and Glu457. The incorrect docking of H12 blocks the corepressor binding surface and also cannot establish the coactivator binding surface. Ligand binding is affected by these mutations indirectly by facilitating water penetration in the active site that destabilizes hydrophobic ligand binding pocket interactions.

Materials and Methods

Plasmid vectors

The construction of plasmids used for the synthesis of TRβ1 (pCMX-hTRβ1) had been previously described.[35,55,56] Vectors encoding TRβ1 with an exchange of isoleucine 280 with lysine or methionine (pCMX-I280K and pCMX-I280M) were donated by Professor Brian West and have been already described.[37] The vectors with mutation of isoleucine 280 to arginine (pCMX-I280R) and with deletion of the last 10 amino acids of TRβ1 (pCMX-F451X) were generated by site-directed mutagenesis (QuickChange Site-Directed Mutagenesis; Stratagene) employing primers containing the required nucleotide sequence. The double mutant I280R/F451X was constructed by adding mutation I280R to pCMX-F451X.

The plasmids for the expression of proteins fused with GST were pGEx (Pharmacia-Upjohn), pGEX-SRC-1 (residues 381–882),[35] pGEX-GRIP-1 (residues 563–767), pGEX-SMRT (residues 987–1491),[56,57] and pGEX-RXR (full),[35] which encode proteins GST, GST-SRC-1, GST-GRIP-1, GST-SMRT, and GST-RXR, respectively. The reporter plasmids containing the elements of positive responses DR4/F2/TREpal-TK-LUC and negatively regulated promoter Δ Coll T_3-LUC[58,59] were donated by Dr. John D. Baxter.

Expression and purification of recombinant proteins in *Escherichia coli*

Proteins fused with GST were expressed in *E. coli* and purified according to the protocol described below: 50 μl of the *E. coli* bacterium strain BL21 was transformed with 1–2 ng of plasmid, pGEX, pGEX-SRC1 (residues 381–882), pGEX-GRIP1 (residues 563–767), or pGEX-SMRT (residues 987–1491), which expresses the respective protein fragments fused to GST. The isolated colony was inoculated in 5 ml of 2× LB medium (preinoculum) and grown for 6–10 h at 22 °C. Subsequently, the preinoculum was split into two bottles containing 500 ml of 2× LB medium with ampicillin. Bacteria were induced with 1 mM IPTG at an OD_{600} of 0.8 for 16 h at 22 °C so that the fusion protein was expressed. After this period, the culture was centrifuged, and the cell pellets were combined and suspended in 20 ml of 1× TST [50 mM Tris (pH 7.5), 150 mM NaCl, and 0.05% Tween 20]. Five hundred microliters of lysozyme (10 mg/ml) was added and incubated on ice for 15 min. Cells were then sonicated (four pulses of 20 s at level 5.5 with a 5-min interval between each pulse). Soon after, the cell lysate was separated by centrifugation at 12,000 rpm for 30 min. Concurrently, 665 μl of glutathione beads was prepared according to the manufacturer's instructions. Briefly, the beads were washed with 5 vol of 1× TST and separated by rapid centrifugation (5000 rpm for 2 min). Then, in order to allow the interaction of beads with the GST, we resuspended the beads in 500 μl of 1× TST and added them to the culture supernatant. This incubation was maintained at 4 °C for 2 h. The beads were collected by centrifugation at 5000 rpm for 5 min and then washed three times with 20 ml of 1× TST. After the beads had been washed, they were resuspended in 600 μl of 1× TST containing 1 mM DTT, 0.5 mM PMSF, 1:1000 protease inhibitor cocktail (Sigma), and 1 ml of glycerol. The beads containing the fusion proteins were stored at −20 °C until their use in GST experiments on protein–protein interaction in solution. GST constructs bound to the resin were quantified with Coomassie Plus Protein Assay Reagent (Pierce) according to the manufacturer's instructions and submitted to sodium dodecyl sulfate–polyacrylamide gel electrophoresis (SDS-PAGE) to assess purity (90–95%).

GST assay (GST pull-down assay)

For these experiments, ^{35}S-labeled TRs were produced *in vitro* with pCMX-TRβ1wt or pCMX mutant vectors using the TNT-Coupled Reticulocyte Lysate System (Promega, Madison, WI) containing a methionine-free amino acid mixture. DNA plasmid (1–2 μg), together with ^{35}S-labeled methionine, was added to the TNT Quick Master Mix and incubated in 50 μl for 90 min at 30 °C. To confirm the efficiency of the translation of ^{35}S-labeled proteins, we submitted the final mixture to SDS-PAGE, dried it, and visualized it by autoradiography. The binding experiments were performed by mixing glutathione-linked Sepharose beads containing 10 μg of GST-SMRT (residues 987–1491), GST-SRC-1 (residues 381–882), and GST-GRIP-1 (residues 563–767) fusion proteins with 3 μl of ^{35}S-labeled wild-type or mutant hTRβ1 in 150 μl of binding buffer (20 mM Hepes, 150 mM KCl, 25 mM $MgCl_2$, 10% glycerol, 1 mM dithiothreitol, 0.2 mM phenylmethylsulfonyl fluoride, and protease inhibitors) containing 2 μg/ml bovine serum albumin for 100 min at 4 °C. After the incubation, the beads were washed three times with 1 ml of binding buffer, and the bound proteins were separated using 10% polyacrylamide gels containing SDS (SDS-PAGE) and visualized by autoradiography.[60]

Cell culture, transfection, and luciferase enzyme activity assays

The procedures for cell culture, transfection, and luciferase enzyme activity assays were performed

according to methods described previously.[61] Human promonocyte (U937) was obtained from the Cell Culture Facility at the University of California, San Francisco. These cells were cultured in RPMI 1640 containing 10% of fetal bovine serum with 2 mM glutamine, 50 μg/ml penicillin, and 50 μg/ml streptomycin, and kept in an incubator at 37 °C in 5% CO_2. The electroporation method was used for the transfection of cells maintained in culture. U937 cells (9 million) were collected by centrifugation and suspended in 0.5 ml of phosphate-buffered saline containing 0.1% of dextrose. These cells were then mixed with 4 μg of reporter plasmid and 0.5 μg of TRβ1 expression vector and then transferred to a cuvette. After storage at room temperature for 5 min, they were electroporated using a pulse generator (Bio-Rad) at 0.3 V and 960 μF. After electroporation, the cells were transferred to fresh media and then plated on 12-well multiplates containing RPMI 1640 with 10% of fetal bovine serum and incubated for 24 h at 37 °C with ethanol (vehicle) or T_3 (10^{-7} M). After 24 h, the cells were collected by centrifugation, lysed by the addition of 150 μl of 1× lysis buffer (Luciferase Assay System; Promega), and assayed for luciferase activity in a luminometer (Turner). Transfection data are expressed as the mean ± standard error of the mean of a minimum of triplicate samples, repeated three to five times. The empty vector pCMX was used as control for transfections without TRβ1.

Site-directed mutagenesis

Mutants I280R, F451X, and I280R/F451X were generated by the PCR site-directed mutagenesis technique (QuickChange Site-Directed Mutagenesis; Stratagene), which employs synthetic oligonucleotides as primers containing the sequence of nucleotides mutated (substitution at an encoder codon of correct amino acid by an encoder of arginine or a stop codon, in the case of F451X). pCMX-hTRβ1 was amplified using high-fidelity plaque-forming unit DNA polymerase enzyme to generate mutant plasmids. The mutated sequence was verified by DNA sequencing (Sequenase; Stratagene).

Trypsin protection assays

Three micrograms of wild-type TRβ1 or mutants synthesized *in vitro* with Met-^{35}S was preincubated with T_3 (10^{-8}, 10^{-7}, and 10^{-6} M) or vehicle (ethanol) for 20 min at room temperature in a final volume of 10 μl of 1× TST. Then trypsin was added (at a concentration of 10 mg/ml in the reaction) for 10 min at 37 °C. The products of the reactions were boiled and analyzed by SDS-PAGE, followed by autoradiography.[20]

T_3 binding assay

TRs were expressed using a kit (TNT T7-Quick Coupled Transcription/Translation System; Promega). T_3 binding affinities were determined using saturating binding assay. Briefly, 15 fM of each synthesized protein *in vitro* was incubated overnight at 4 °C with varying concentrations of T_3 labeled with ^{125}I (PerkinElmer Life Sciences) in 100 μl of E400 buffer [400 mM NaCl, 20 mM K_3PO_4 (pH 8), 0.5 mM ethylenediaminetetraacetic acid, 1.0 mM $MgCl_2$, and 10% of glycerol], 1 mM monothioglycerol, and 50 μg of calf thymus histones (Calbiochem). T_3-^{125}I was isolated by gravity through a 2-ml Sephadex G-25 column (Amersham Biosciences) and quantified in a γ-counter (COBRA; Packard Instruments). The binding curves were fitted by nonlinear regression, and the binding dissociation constants (K_d) were calculated using the one-site saturation binding model and one-phase exponential decay, respectively, present in the PRISM program, version 4.0 (GraphPad Software, Inc., San Diego, CA).

Statistical analysis

All results presented here represent the mean and standard deviation of at least four independent experiments. All statistical analyses and graphics were performed using the PRISM program, version 4.0 (GraphPad Software, Inc.). The statistical analysis test used in the experiments was analysis of variance, followed by Tukey test. Results were considered statistically different when the p value was smaller than 0.05. The differences or similarities are represented in the form of letters (a, b, c, and d) over the bars. Different letters indicate significant differences between the groups, and identical letters indicate that there is no statistical difference.

MD simulations

The initial protein structure was the LBD of wild-type TRβ1 bound to T_3, obtained by our research group [Protein Data Bank (PDB) ID: 3GWS].[62] Missing Ω-loop (residues 253–262) was modeled based on the corresponding region of wild-type TRα–LBD (PDB ID: 2H79).[62] The complete simulated systems—containing TRβ1–LBD, water, and one counterion for each charged residue for electroneutrality—were built with Packmol.[63,64] We use a cubic box with 16,600 water molecules with side dimensions of 81 Å. For the simulation of mutant structures, the simulation box of the wild-type structure was used, and the side chain of residue 280 was substituted with the *psfgen* program.[65,66] For I280K and I280R, a random water molecule was replaced by a chloride ion to maintain electroneutrality. Four systems were therefore built: wild-type TRβ1, I280M, I280K, and I280R.

MD simulations were performed with NAMD[65,66] by applying periodic boundary conditions and CHARMM parameters.[67] The TIP3P model was used for water.[68] T_3 parameters had been reported previously.[22] A time step of 2.0 fs was used, and all hydrogen-to-heavy-atom bonds were kept rigid. A 14-Å cutoff with smooth switching function starting at 12 Å was used for van der Waals interactions, whereas electrostatic forces were treated via the particle mesh Ewald method.[69]

Energy minimization and equilibration were performed independently for each system, as follows: total energies were minimized by 700 conjugate gradient (CG) steps keeping all protein atoms fixed, except for the modeled regions, which were always allowed to move. Fixing only the C^{α} atoms, we performed another 500 CG steps. Finally, 300 CG steps were carried out without any restrictions. After minimization, 4-ns MD simulations were performed under conditions of constant temperature

and pressure (NpT ensemble) at 298 K and 1 bar, with a Langevin damping coefficient of 5 ps^{-1} and with Langevin piston controlled using a period of 200 fs and a decay of 100 fs. Atomic coordinates and NAMD files for MD simulations are available from the authors upon request.

The temporal variations of the structural properties of the protein were computed with the objective of determining the relaxation and stability of TR–LBDs, in particular of mutants constructed from the wild-type structure. The chosen structural properties were as follows: RMSDs of the Cα atoms, RMSD; radius of gyration R_g; percentage of native contacts, % N_{cont}; percentage of secondary structure, % N_{sec} (for more details, see Martínez *et al.*[70]). The initial structure of the simulations was used as reference in these calculations. It was found that the mutants lead to small losses of secondary structure and native contacts, and small increases in RMSDs. All global structural properties have converged within 2 ns. Thus, the first 2 ns of the simulations was not used for the analysis. Analyses were performed for the last 2 ns of the trajectory using VMD[71] and our home-made programs†.

Acknowledgements

The authors thank the following Brazilian agencies for financial support: Fundação de Amparo a Pesquisa do Estado de São Paulo, Conselho Nacional de Desenvolvimento Científico e Tecnológico (Grants 476895/2008-1 and 620195/2008), and Coordenação de Aperfeiçoamento de Pessoal de Nível Superior.

References

1. Wagner, R. L., Apriletti, J. W., McGrath, M. E., West, B. L., Baxter, J. D. & Fletterick, R. J. (1995). A structural role for hormone in the thyroid hormone receptor. *Nature*, **378**, 690–697.
2. Borngraeber, S., Budny, M. J., Chiellini, G., Cunha-Lima, S. T., Togashi, M., Webb, P. *et al.* (2003). Ligand selectivity by seeking hydrophobicity in thyroid hormone receptors. *Proc. Natl Acad. Sci. USA*, **100**, 15358–15363.
3. Webb, P. (2004). Selective activators of thyroid hormone receptors. *Expert Opin. Invest. Drug*, **13**, 489–500.
4. Ribeiro, R. C. J., Kushner, P. J. & Baxter, J. D. (1995). The nuclear hormone receptor gene superfamily. *Annu. Rev. Med.* **46**, 443–453.
5. McKenna, N. J. & O'Malley, B. W. (2002). Combinatorial control of gene expression by nuclear receptors and coregulators. *Cell*, **108**, 465–474.
6. Pelton, P. D., Patel, M. & Demarest, K. T. (2005). Nuclear receptors as potential targets for modulating reverse cholesterol transport. *Curr. Top. Med. Chem.* **5**, 265–281.
7. Nettles, K. W. & Greene, G. L. (2005). Ligand control of coregulator recruitment to nuclear receptors. *Annu. Rev. Physiol.* **67**, 309–333.
8. Weatherman, R. V., Fletterick, R. J. & Scanlan, T. S. (1999). Nuclear-receptor ligands and ligand-binding domains. *Annu. Rev. Biochem.* **68**, 559–581.
9. Bourguet, W., Germain, P. & Gronemeyer, H. (2000). Nuclear receptor ligand-binding domains: three-dimensional structures, molecular interactions and pharmacological implications. *Trends Pharmacol. Sci.* **21**, 381–388.
10. Gronemeyer, H., Gustafsson, J. A. & Laudet, V. (2004). Principles for modulation of the nuclear receptor superfamily. *Nat. Rev. Drug Discov.* **3**, 950–964.
11. Bourguet, W., Ruff, M., Chambon, P., Gronemeyer, H. & Moras, D. (1995). Crystal structure of the ligand-binding domain of the human nuclear receptor RXR-alpha. *Nature*, **375**, 377–382.
12. Renaud, J. P., Rochel, N., Ruff, M., Vivat, V., Chambon, P., Gronemeyer, H. *et al.* (1995). Crystal structure of the RAR-γ ligand binding domain bound to all-*trans* retinoic acid. *Nature*, **378**, 681–689.
13. Nolte, R. T., Wisely, G. B., Westin, S., Cobb, J. E., Lambert, M. H., Kurokawa, R. *et al.* (1998). Ligand binding and co-activator assembly of the peroxisome proliferator activated receptor gamma. *Nature*, **395**, 137–143.
14. Baker, K. D., Shewchuk, L. M., Kozlova, T., Makishima, M., Hassell, A., Wisely, B. *et al.* (2003). The *Drosophila* orphan nuclear receptor DHR38 mediates an atypical ecdysteroid signaling pathway. *Cell*, **113**, 731–742.
15. Greschik, H., Flaig, R., Renaud, J. P. & Moras, D. (2004). Structural basis for the deactivation of the estrogen-related receptor gamma by diethylstilbestrol or 4-hydrotamoxifen and determinants of selectivity. *J. Biol. Chem.* **279**, 33639–33646.
16. Kallen, J., Schlaeppi, J. M., Bitsch, F., Filipuzzi, I., Schlib, A., Riou, V. *et al.* (2004). Evidence for ligand independent transcriptional activation of the human estrogen-related receptor alpha (ERR alpha)—crystal structure of ERR alpha ligand binding do REFER main in complex with peroxisome proliferator-activated receptor coactivator-1 alpha. *J. Biol. Chem.* **279**, 49330–49337.
17. Wang, L., Zuercher, W. J., Consler, T. G., Lambert, M. H., Miller, A. B., Orband-Miller, L. A. *et al.* (2006). X-ray crystal structures of the estrogen-related receptor-gamma ligand binding domain in three functional states reveal the molecular basis of small molecule regulation. *J. Biol. Chem.* **281**, 37773–37781.
18. Johnson, B. A., Wilson, E. M., Li, Y., Moller, D. E., Smith, R. G. & Zhou, G. (2000). Ligand-induced stabilization of PPARγ monitored by NMR spectroscopy: implications for nuclear receptor activation. *J. Mol. Biol.* **298**, 187–194.
19. Pissios, P., Tzameli, I., Kushner, P. J. & Moore, D. D. (2000). Dynamic stabilization of nuclear receptor ligand binding domains by hormone or corepressor binding. *Mol. Cell*, **2**, 245–253.
20. Gee, A. C. & Katzenellenbogen, J. A. (2001). Probing conformational changes in the estrogen receptor: evidence for a partially unfolded intermediate facilitating ligand binding and release. *Mol. Endocrinol.* **15**, 421–428.

† http://lm-mdanalysis.googlecode.com

21. Kallenberger, B. C., Love, J. D., Chatterjee, V. K. & Schwabe, J. W. (2003). A dynamic mechanism of nuclear receptor activation and its perturbation in a human disease. *Nat. Struct. Biol.* **10**, 136–140.
22. Martínez, L., Sonoda, M. T., Webb, P., Baxter, J. D., Skaf, M. S. & Polikarpov, I. (2005). Molecular dynamics simulations reveal multiple pathways of ligand dissociation from thyroid hormone receptors. *Biophys. J.* **89**, 2011–2023.
23. Martínez, L., Webb, P., Polikarpov, I. & Skaf, M. S. (2006). Molecular dynamics simulations of ligand dissociation from thyroid hormone receptors: evidence of the likeliest escape pathway and its implications for the design of novel ligands. *J. Med. Chem.* **49**, 23–26.
24. Sonoda, M. T., Martínez, L., Webb, P., Skaf, M. S. & Polikarpov, I. (2008). Ligand dissociation from estrogen receptor is mediated by receptor dimerization: evidence from molecular dynamics simulations. *Mol. Endocrinol.* **22**, 1565–1578.
25. Martínez, L., Polikarpov, I. & Skaf, M. S. (2008). Only subtle protein conformational adaptations are required for ligand binding to thyroid hormone receptors: simulations using a novel multipoint steered molecular dynamics approach. *J. Phys. Chem. B*, **112**, 10741–10751.
26. McGee, T. D., Edwards, J. & Roitberg, A. E. (2008). Preliminary molecular dynamics simulations of estrogen receptor α ligand binding domain from antagonist to apo. *Int. J. Environ. Res. Public Health*, **5**, 111–114.
27. Zhou, J., Liu, B., Geng, G. & Wu, J. H. (2010). Study of the impact of the T877A mutation on ligand-induced helix-12 positioning of the androgen receptor resulted in design and synthesis of novel antiandrogens. *Proteins*, **78**, 623–637.
28. Yan, X., Broderick, D., Leid, M. E., Schimerlik, M. I. & Deinzer, M. L. (2003). Dynamics and ligand-induced solvent accessibility changes in human retinoid X receptor homodimer determined by hydrogen deuterium exchange and mass spectrometry. *Biochemistry*, **43**, 909–917.
29. Hamuro, Y., Coales, S. J., Morrow, J. A., Molnar, K. S., Tuske, S. J., Southern, M. R. *et al.* (2006). Hydrogen/deuterium exchange (H/D-Ex) of PPARλ LBD in the presence of various modulators. *Protein Sci.* **15**, 1883–1892.
30. Frego, L. & Davidson, W. (2006). Conformational changes of the glucocorticoid receptor ligand binding domain induced by ligand and cofactor binding, and the location of cofactor binding sites determined by hydrogen/deuterium exchange mass spectrometry. *Protein Sci.* **15**, 722–730.
31. Yan, X., Pérez, E., Leid, M., Schimerlik, M. I., de Lera, A. R. & Deinzer, M. L. (2007). Deuterium exchange and mass spectrometry reveal the interaction differences of two synthetic modulators of RXR LBD. *Protein Sci.* **16**, 2491–2501.
32. Chandra, V., Huang, P., Hamuro, Y., Raghuram, S., Wang, Y., Burris, T. P. *et al.* (2008). Structure of the intact PPAR-λ–RXR-α nuclear receptor complex on DNA. *Nature*, **456**, 350–356.
33. Dai, S. Y., Burris, T. P., Dodge, J. A., Montrose-Rafizadeh, C., Wang, Y., Pascal, B. D. *et al.* (2009). Unique ligand binding patterns between estrogen receptor A and β revealed by hydrogen deuterium exchange. *Biochemistry*, **48**, 9668–9676.
34. Figueira, A. C. M., Saidemberg, D. M., Souza, P. C. T., Martínez, L., Scanlan, T. S., Baxter, J. D. *et al.* (2011). Analysis of agonist and antagonist effects on thyroid hormone receptor conformation by hydrogen/deuterium exchange. *Mol. Endocrinol.* **25**, 15–31.
35. Feng, W., Ribeiro, R. C. J., Wagner, R. L., Nguyen, H., Apriletti, J. W., Fletterick, R. J. *et al.* (1998). Hormone-dependent coactivator binding to a hydrophobic cleft on nuclear receptors. *Science*, **280**, 1747–1749.
36. Webb, P., Anderson, C. M., Valentine, C., Nguyen, P., Marimuthu, A., West, B. L. *et al.* (2000). The nuclear receptor corepressor (N-CoR) contains three isoleucine motifs (I/LXXII) that serve as receptor interaction domains (IDs). *Mol. Endocrinol.* **14**, 1976–1985.
37. Marimuthu, A., Feng, W., Tagami, T., Nguyen, H., Jameson, J. L., Fletterick, R. J. *et al.* (2002). TR surfaces and conformations required to bind nuclear receptor corepressor. *Mol. Endocrinol.* **16**, 271–286.
38. Frank-Raue, K., Lorenz, A., Haag, C., Hoppner, W., Boll, H. U., Knorr, D. *et al.* (2004). Severe form of thyroid hormone resistance in a patient with homozygous/hemizygous mutation of T_3 receptor gene. *Eur. J. Endocrinol.* **150**, 819–823.
39. Margotat, A., Sarkissian, G., Malezet-Desmoulins, C., Peyrol, N., Guillem, V. V., Wemeau, J. L. *et al.* (2001). Identification of eight new mutations in the c-erbA beta gene of patients with resistance to thyroid hormone. *Ann. Endocrinol.* **62**, 220–225.
40. Tagami, T., Gu, W. X., Peairs, P. T., West, B. L. & Jameson, J. L. (1998). A novel natural mutation in the thyroid hormone receptor defines a dual functional domain that exchanges nuclear receptor corepressors and coactivators. *Mol. Endocrinol.* **12**, 1888–1902.
41. Olateju, T. & Vanderpump, M. P. J. (2006). Thyroid hormone resistance. *Ann. Clin. Biochem.* **46**, 431–440.
42. Miyoshi, Y., Nakamura, H., Tagami, T., Sasaki, S., Dorin, R. I., Taniyama, M. *et al.* (1998). Comparison of the functional properties of three different truncated thyroid hormone receptors identified in subjects with resistance to thyroid hormone. *Mol. Cell Endocrinol.* **137**, 169–176.
43. Darimont, B. D., Wagner, R. L., Apriletti, J. W., Stallcup, M. R., Kushner, P. J., Baxter, J. D. *et al.* (1998). Structure and specificity of nuclear receptor–coactivator interactions. *Genes Dev.* **12**, 3343–3356.
44. Nettles, K. W., Bruning, J. B., Gil, G., Nowak, J., Sharma, S. K., Hahm, J. B. *et al.* (2008). NFκB selectivity of estrogen receptor ligands revealed by comparative crystallographic analyses. *Nat. Chem. Biol.* **4**, 241–247.
45. Carlson, K. E., Choi, I., Gee, A., Katzenellenbogen, B. S. & Katzenellenbogen, J. A. (1997). Altered ligand binding properties and enhanced stability of a constitutively active estrogen receptor: evidence that an open pocket conformation is required for ligand interaction. *Biochemistry*, **36**, 14897–14905.
46. Weis, K. E., Ekena, K., Thomas, J. A., Lazennec, G. & Katzenellenbogen, B. S. (1996). Constitutively active human estrogen receptors containing amino acid substitutions for tyrosine 537 in the receptor protein. *Mol. Endocrinol.* **10**, 1388–1398.

47. Farboud, B. & Privalsky, M. L. (2003). Retinoic acid receptor-α is stabilized in a repressive state by its C-terminal, isotype-specific F domain. *Mol. Endocrinol.* **18**, 2839–2853.
48. Hauksdottir, H., Farboud, B. & Privalsky, M. L. (2003). Retinoic acid receptors β and λ do not repress, but instead activate target gene transcription in both the absence and presence of hormone ligand. *Mol. Endocrinol.* **17**, 373–385.
49. Gurnell, M., Wentworth, J. M., Agostini, M., Adams, M., Collingwood, T. N., Provenzano, C. *et al.* (2000). A dominant-negative peroxisome proliferator-activated receptor λ (PPARλ) mutant is a constitutive repressor and inhibits PPARλ-mediated adipogenesis. *J. Biol. Chem.* **275**, 5754–5759.
50. Claudia ProvenzanoBleicher, L., Aparício, R., Nunes, F. M., Martinez, L., Gomes Dias, S. M., Figueira, A. C. *et al.* (2008). Structural basis of GC-1 selectivity for thyroid hormone receptor isoforms. *BMC Struct. Biol.* **8**, 1–13.
51. Martínez, L., Nascimento, A. S., Nunes, F. M., Phillips, K., Aparício, R., Dias, S. M. *et al.* (2009). Gaining ligand selectivity in thyroid hormone receptors via entropy. *Proc. Natl Acad. Sci. USA*, **106**, 20717–20722.
52. Horn, F., Lau, A. L. & Cohen, F. E. (2004). Automated extraction of mutation data from the literature: application of MuteXt to G protein-coupled receptors and nuclear hormone receptors. *Bioinformatics*, **20**, 557–568.
53. Chen, S., Johnson, B. A., Li, Y., Aster, S., McKeever, B., Mosley, R. *et al.* (2000). Both coactivator LXXLL motif-dependent and -independent interactions are required for peroxisome proliferator-activated receptor gamma (PPARgamma) function. *J. Biol. Chem.* **275**, 3733–3736.
54. Zhang, Z. P., Hutcheson, J. M., Poynton, H. C., Gabriel, J. L., Soprano, K. J. & Soprano, D. R. (2003). Arginine of retinoic acid receptor beta which co-ordinates with the carboxyl group of retinoic acid functions independent of the amino acid residues responsible for retinoic acid receptor subtype ligand specificity. *Arch. Biochem. Biophys.* **409**, 375–384.
55. Umesono, K., Murakami, K. K., Thompson, C. C. & Evans, R. M. (1991). Direct repeats as selective response elements for thyroid hormone, retinoic acid, and vitamin D3 receptors. *Cell*, **28**, 1255–1266.
56. Webb, P., Nguyen, P. & Kushner, P. J. (2003). Differential SERM effects on corepressor binding dictate ERα activity *in vivo*. *J. Biol. Chem.* **278**, 6912–6920.
57. Lopez, G., Schaufele, F., Webb, P., Holloway, J. M., Baxter, J. D. & Kushner, P. J. (1993). Positive and negative modulation of Jun action by thyroid hormone receptor at a unique AP1 site. *Mol. Cell. Biol.* **13**, 3042–3049.
58. Guissouma, H., Dupré, S. M., Becker, N., Jeannin, E., Seugnet, I., Desvergne, B. *et al.* (2002). Feedback on hypothalamic TRH transcription is dependent on thyroid hormone receptor N terminus. *Mol. Endocrinol.* **16**, 1652–1666.
59. Santos, G. M., Afonso, V., Barra, G. B., Togashi, M., Webb, P., Neves, F. R. A. *et al.* (2006). Negative regulation of superoxide dismutase-1 promoter by thyroid hormone. *Mol. Pharmacol.* **70**, 793–800.
60. Laemmli, U. K. (1970). Cleavage of structural proteins during the assembly of the head of bacteriophage T4. *Nature*, **15**, 680–685.
61. Chiellini, G., Apriletti, J. W., Yoshihara, H. A., Baxter, J. D., Ribeiro, R. C. & Scanlan, T. S. (1998). A high-affinity subtype-selective agonist ligand for the thyroid hormone receptor. *Chem. Biol.* **5**, 299–306.
62. Nascimento, A. S., Dias, S. M. G., Nunes, F. M., Aparício, R., Ambrosio, A. L. B., Bleicher, L. *et al.* (2006). Structural rearrangements in the thyroid hormone receptor hinge domain and their putative role in the receptor function. *J. Mol. Biol.* **360**, 586–598.
63. Martínez, J. M. & Martínez, L. (2003). Packing optimization for automated generation of complex system's initial configurations for molecular dynamics and docking. *J. Comput. Chem.* **24**, 819–825.
64. Martínez, L., Andrade, R., Birgin, E. G. & Martínez, J. M. (2009). A package for building initial configurations for molecular dynamics simulations. *J. Comput. Chem.* **30**, 2157–2164.
65. Kalé, L., Skeel, R., Bhandarkar, M., Brunner, R., Gursoy, A., Krawetz, N. *et al.* (1999). NAMD2: greater scalability for parallel molecular dynamics. *J. Comput. Phys.* **151**, 283–312.
66. Phillips, J. C., Braun, R., Wang, W., Gumbart, J., Takhorshid, E., Villa, E. *et al.* (2005). Scalable molecular dynamics with NAMD. *J. Comput. Chem.* **26**, 1781–1802.
67. MacKerell, A. D., Bashford, D., Bellott, M., Dunbrack, R. L., Evanseck, J. D., Field, M. J. *et al.* (1998). All-atom empirical potential for molecular modeling and dynamics studies of proteins. *J. Phys. Chem. B*, **102**, 3586–3616.
68. Jorgensen, W. L., Chandrasekhar, J., Madura, J. D., Impey, R. W. & Klein, M. L. (1983). Comparison of simple potential functions for simulating liquid water. *J. Chem. Phys.* **79**, 926–935.
69. Darden, T., York, D. & Pedersen, L. (1993). Particle mesh Ewald: an $N\cdot\log(N)$ method for Ewald sums in large systems. *J. Chem. Phys.* **98**, 10089–10092.
70. Martínez, L., Souza, P. C. T., Garcia, W., Batista, F. A., Portugal, R. V., Nascimento, A. S. *et al.* (2010). On the denaturation mechanisms of the ligand binding domain of thyroid hormone receptors. *J. Phys. Chem. B*, **114**, 1529–1540.
71. Humphrey, W., Dalke, A. & Schulten, K. (1996). VMD—Visual Molecular Dynamics. *J. Mol. Graphics*, **14**, 33–38.